Proceedings of the West Virginia Academy of Science

Original Research Paper

A Simple and Inexpensive Downdraft Table to Limit Aerosol Exposure from Patients, Aerosol-Generating Procedures, and Surgical Smoke

Matthew J. Zdilla, D.C.[1*]; W. Travis Goldsmith, M.S.[2,3]; Timothy R. Nurkiewicz, Ph.D. [2,3]

1. Department of Pathology, Anatomy, and Laboratory Medicine (PALM), West Virginia University School of Medicine, Morgantown, WV, USA

2. Department of Physiology and Pharmacology, West Virginia University School of Medicine, Morgantown, WV, USA

3. Center for Inhalation Toxicology, West Virginia University School of Medicine, Morgantown, WV, USA

Article history

Received: 18 January 2023

Revised: 29 March 2023

Accepted: 30 March 2023

**Corresponding Author*: Dr. Matthew J. Zdilla, Department of Pathology, Anatomy, and Laboratory Medicine (PALM), West Virginia University School of Medicine, Robert C. Byrd Health Sciences Center, Morgantown, West Virginia, 26506 (USA)
Email: matthew.zdilla@hsc.wvu.edu

Abstract: Pathogenic aerosols are common, especially in clinical settings. Aerosols are released from quiet and forced respiration, non-respiratory movements (e.g., coughing and sneezing), aerosol-generating procedures, and surgical smoke plumes. Aerosols may contain viruses (e.g., coronaviruses, influenza viruses, adenoviruses) and bacteria (e.g., *Streptococcus pneumoniae*, *Stapylococcus aureus*, *Pseudomonas aeruginosa*, *Mycobacterium tuberculosis*). Surgical smoke plumes may contain harmful volatile organic compounds (e.g., formaldehyde), viral particles (e.g., human papillomavirus), or cancerous cells. Thus, the containment of airborne pathogenic organisms, xenobiotics, and bioaerosols is of the utmost importance. Yet, despite the importance of negative airflow and exhaust ventilation, many clinical environments do not have adequate ventilation systems— often due to significant monetary expenses or other barriers to access such as remote locations. Recently, a relatively inexpensive downdraft table (< 200 USD), made of wood, tarps, rebar, and corrugated steel roofing material and a simple local exhaust ventilation system (~ 300 USD) have been demonstrated to eliminate airborne VOCs, including VOCs found in surgical smoke. However, the table has not been assessed regarding the capacity to remove water-based aerosols. Therefore, the purpose of this research was to assess the ability of the downdraft table and local exhaust ventilation system to exhaust varied water-based and organic aerosols. The study identifies that a simple and inexpensive downdraft table can effectively exhaust aerosols like those found in clinical environments. This study represents an innovation in accessible medical technology that will improve health and safety in regions that include developing countries and remote locations.

Keywords: aerosol; aerosol-generating procedure; occupational safety; ventilation; surgery

Introduction

The global severe acute respiratory syndrome coronavirus 2 (SARS-CoV-2) pandemic (i.e., COVID-19 pandemic) has prompted renewed interest in the containment of airborne pathogens, including aerosolized pathogens from so-called "aerosol-generating procedures." The ever-growing list of aerosol-generating procedures includes dental procedures, tracheal intubation / extubation, tracheostomy, thoracostomies, oropharyngeal/tracheal aspiration, high-flow air/oxygen delivery, chest compression / cardiopulmonary resuscitation, general anesthesia, and varied endoscopic procedures such as bronchoscopy, esophagogastroduodenoscopy, trans-esophageal echocardiography, and retrograde

cholangiopancreatography, as well as surgery, in general (Hellman et al., 2020; Klompas et al., 2021; Tkacik et al., 2021; Romanzi et al., 2021; Donato et al., 2021; Jain et al., 2021; Komperda et al., 2021). Further, exertional breathing (e.g., exercise stress testing, labor), coughing, sneezing, forced expiratory maneuvers, spirometry, and varied respiratory therapy activities also increase the risk of airborne pathogen spread (Wilson et al., 2021, Klompas et al., 2021).

Invasive procedures utilizing lasers or electrosurgical equipment (e.g., electrocautery, laser surgery, utilization of ultrasonic scalpels) generate aerosols in the form of surgical smoke and are thus implicated in the airborne spread of viral particles (e.g., from the treatment of venereal warts), cancerous cells, harmful volatile organic compounds (VOCs) (Alp et al., 2006; Ulmer, 2008; Lee et al., 2018; Mowbray et al., 2020; Occupational Safety and Health Administration, 2021). Indeed, depending on exposure, health risks regarding surgical smoke include emphysema, asthma, bronchitis, headache, irritation to eyes/nose/throat, sneezing, nausea, vomiting, weakness, lightheadedness, dermatitis, nasopharyngeal lesions, cardiovascular dysfunction, hepatitis, human immunodeficiency virus infection, and varied cancers (e.g., carcinoma and leukemia) (Alp et al., 2006). Because bioaerosols produce diverse and significant health risks and increase the likelihood for adverse clinical outcomes, there is a demand for robust protection and containment measures.

Adequate airflow and exhaust ventilation are necessary to eliminate pathogens and harmful aerosols in order to prevent nosocomial infection and disease in the clinical environment. Precautions to limit the spread of airborne pathogens during aerosol-generating procedures include the utilization of airborne infection isolation rooms with negative airflow as well as local exhaust ventilation systems (e.g., smoke evacuators) (Ulmer, 2008; Klompas et al., 2021). Yet, despite the importance of negative airflow and exhaust ventilation, many clinical environments do not have adequate ventilation systems— often due to significant monetary expenses or other barriers to access such as remote locations (Bhattacharjee et al., 2021).

Recently, a relatively inexpensive downdraft table (< 200 USD), made of wood, tarps, rebar, and corrugated steel roofing material and simple local exhaust ventilation systems (~ 300 USD) have been demonstrated to eliminate airborne VOCs, including VOCs found in surgical smoke (e.g., aldehydes and phenol) including known carcinogens (e.g., formaldehyde) (Zdilla, 2020, 2021, and 2022). The table also handled a load of at least 331 kg without damage and generated an exhaust flow of 3099 m^3/hr (Zdilla, 2022). It was posited that the downdraft table, paired with a local exhaust ventilation system, might also effectively eliminate varied water vapors, smokes containing organic compounds, and other aerosols. Thus, the downdraft system may have broad and important clinical value, particularly in economically depressed regions (i.e., developing countries), remote field locations, and in scenarios of quarantine and hospital patient overflow (Zdilla, 2022). Therefore, the purpose of this study was to assess the ability of the downdraft table and local exhaust ventilation system to exhaust varied water-based and organic aerosols; accordingly, the study determines the range of physical parameters of operation and their effectiveness in containing aerosols.

Materials and Methods

A downdraft table made of lumber, oriented strand board, tarps, staples, rebar, galvanized corrugated steel, and duct take-offs was used in this study (Figure 1). The downdraft table was identical to that recently described by Zdilla (2022). The table had a length of 221 cm, a width of 93 cm, height of 24 cm, and weight of 75 kg. The downdraft table was affixed to five VIVOSUN 6-inch 440 cfm inline duct fans (VIVOSUN; Los Angeles, CA) via flexible ducting which led to the exterior of a building through a window in five configurations that resembled the “Type A” local exhaust ventilation systems of recent reports (Zdilla, 2020, 2021, 2022). Duct tape was used to seal narrow openings in the casings of the in-line duct fans. Likewise, duct tape was used to prevent re-entrainment of vapors through narrow openings at the window. For additional precaution, towels and blankets were used to ensure that any vapors that might leak from small openings in flexible ducting, fan casing, or vapors that might be re-entrained would be suppressed (Figure 1).

Figure 1. The downdraft table and local exhaust ventilation system. (A) An air conditioning unit was removed from its casing and a piece of oriented strand board with five holes to accommodate 6-inch flexible ducting (diameter ~15 cm) was affixed to the casing. **(B)** Flexible ducting was affixed to 6-inch inline duct fans which were wrapped with duct tape to prevent vapors from exiting seams in the fan casing. **(C)** The downdraft table was placed atop two carts and joined to the flexible ducting. Ducting, fans, and the retrofitted window casing were covered with towels and blankets as an added precaution to ensure that vapors would not spread into the room from any potential leaks in the system.

Air flow was assessed with a HoldPeak® 866B digital anemometer (Zhuhai JiDa Huapu instrument Co., Ltd.; Zhuhai, China; Resolution: 0.1 m/s, 19 ft/min; Accuracy: ±5%).

Several different types of aerosols were generated and visualized with and without the utilization of downdraft in a multifaceted approach. The varied experiments were as follows:

1. Assessment of water vapor produced from condensation occurring post-sublimation of dry ice:

Aerosol emission from quiet breathing was approximated by using dry ice to produce a flow of water vapor. A container, measuring 28 cm in length × 23 cm in width × 27 cm in height, was filled with 4 kg of dry ice (i.e., solid carbon dioxide). The container was positioned centrally upon the surface of the downdraft table. Then, 1000 ml of 48° C water was poured into the container. Thus, the accelerated sublimation of frozen carbon dioxide condensed the humid air into a cold visible fog (combination of invisible carbon dioxide and visible condensed water). The production of the fog was video recorded. The location of the fog in relation to the boundaries of the downdraft table, as well as the elevation of the fog in relation to the table surface, was observed and characterized in both the absence and presence of downdraft ventilation. The process was repeated with the container positioned in the center of the head and foot of the table.

2. Assessment of an aerosolized 35% triethylene glycol + water mixture from fog machines:

Aerosol emission from exertional breathing, non-respiratory air movements (e.g., coughing, sneezing), and aerosol-generating procedures was approximated by ejecting water-based aerosols from fog machines. Two 500-watt fog machines with a 2000-3000 cfm flow and 2-3 m fog-distance (IPHUNGO and AGPTEK Fog Machines; Shenzhen Mambate Industry Development Co., Ltd. China) were filled with a water-based fluid mixture composed of 35% triethylene glycol (FogWorx HD Extreme High-Density Fog Juice; Model Number: 4334422280). The fog machines were placed upon the table in varied arrangements (directed toward one another in the center of the table, directed along the length of the table with parallel trajectory, directed along the length of the table with anti-parallel trajectory, and directed along the width of the table with parallel trajectory). The fog machines function to aerosolize and fluid mixture by heat and, likewise, eject the fog at a relatively fast velocity. The emission of the fog was video recorded. The location of the fog in relation to the boundaries of the downdraft table, as well as the elevation of the fog in relation to the table surface, was observed, video recorded, and characterized in both the absence and presence of downdraft ventilation.

3. Assessment of an aerosolized glycerin + water mixture from a hand-held fog generator:

Aerosols from surgical smoke plumes as well as aerosols emitted from quiet breathing directed away from the table surface were modeled by using a water-based fog with a tendency to travel upward. A hand-held fog generator was filled with a water-based glycerin fluid mixture (Wizard Stick and Super Fluid, Zero Toys Inc. / Quickpoint, Inc. 23 Bradford St. #2, Concord MA 01742). Properties of the fluid include a specific gravity of 1.075 @ 68° F. / 20° C,

vapor pressure of < .025 mm Hg, and vapor density: of 4.1 (water = 1.0). The fog is generated by a heating element within the hand-held device. The device was positioned in centrally upon the surface of the downdraft table and manually operated in both the absence and presence of downdraft ventilation. Light emitting diodes were used to aid in the visualization of the fog. The location of the fog in relation to the boundaries of the downdraft table, as well as the elevation of the fog in relation to the table surface, was observed, video recorded, and characterized.

4. Assessment of cool water vapor generated from an ultrasonic air humidifier:

Aerosol emission from exertional breathing directed over the side of table was approximated by generating water vapor with an ultrasonic humidifier that blows the water vapor with a built-in fan. A cool mist ultrasonic air humidifier (Pure Enrichment MistAire; Model: PEHUMIDIF) with a mist output of 150 ml/h (high setting), intrinsic fan, and directional flow nozzle was used to assess water vapor movement. The humidifier had a height of 23 cm (the height at which the mist exits the machine). The humidifier was positioned near the edge of the table, at the center of the length of the table. The directional flow nozzle was directed tangential to the long axis of the table in order to direct mist flow beyond the perimeter boundary of the table. The mist was backlit by light emitting diodes for visualization and video recorded in both the absence and presence of downdraft ventilation.

5. Assessment of fire and smoke produced from the combustion of matches:

The capacity of the downdraft table to direct flames, extinguish flames, and downdraft smoke was assessed by using matches (Diamond, Model: 4878982123; Royal Oak Enterprises, LLC, 1 Royal Oak Ave, Roswell, GA 30076) composed of poplar extract (88.80% by weight), water, quartz, maize starch, zinc oxide, glue, colloidal silicon dioxide, wollastonite, chromate, anthraquinone, potassium dichromate, sodium sulfate, plaster of Paris, glass fiber, and phosphorus. Varied quantities of matches (a single match, a group of six matches, and a group of ten matches) were ignited and held in an "inverted" position (i.e., flame-end oriented downward) at varied heights above an opening within the surface of the downdraft table. Fire behavior and smoke movement were observed, video recorded, and characterized.

6. Identification of a three-dimensional downdraft ceiling with smoke generated from the combustion of a cellulose / stearic acid wick:

To approximate the distance from the table surface from which a surgical smoke could be downdrafted (hence referred to as the *downdraft ceiling*), and to assess the general variation in aerosol movement above the surface of the table, a smoke pen was used to detect a downdraft ceiling matrix. String was used to plot a matrix of equal sized squares upon the surface of the downdraft table

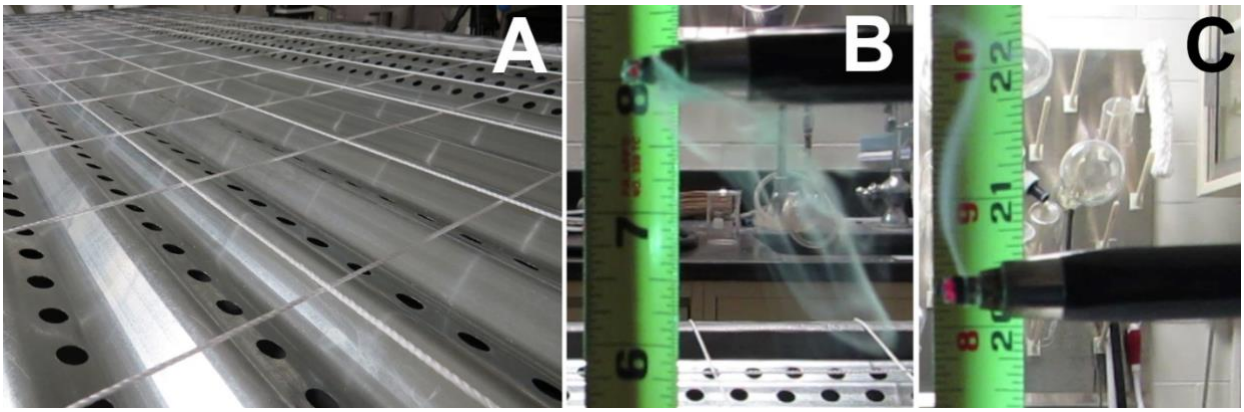

Figure 2: Methodology for the determination of the downdraft ceiling. (A) A matrix of equal sized squares was plotted upon the downdraft table surface with string. Above the center of each square, a measurement of downdraft ceiling height was determined by assessing the direction of smoke emitted from a smoke pen that was gradually elevated above the surface of the table. **(B)** A smoke pen, oriented horizontally alongside a tape measure, is seen emitting a steady stream of smoke that is moving downward, toward the surface of the table. **(C)** The stream of smoke emitted from the smoke pen is seen moving upward and away from the table. The height at which the smoke stream moved upward was recorded for each square of the grid in order to determine a three-dimensional downdraft ceiling.

(Figure 2). The squares measured approximately 13 × 13 cm, thus giving a grid of 16 × 7 squares (112 total). A tape measure was positioned in the center of a square and held above the table in order to measure height above the table surface. A Regin S220 Smoke Pen (BJÖRNAX AB, Ringshyttan Gruvstugan 729 SE-71393 Nora, Sweden) with compatible wicks (Model Number S221) composed of cellulose (80-100%) and stearic acid (6-10%) was ignited and extinguished, as per the manufacturer's guidelines, in order to produce a stream of visible smoke. The smoke pen was held parallel to the long axis of the table (i.e., horizontal to the ground) and slowly elevated in proximity to the tape measure. The smoke was assessed alongside the tape measure to determine the height from the surface of the table at which the smoke formed a stream that moved up (Figure 2). The height was recorded regarding the location upon the table grid.

Regarding statistical analysis of the downdraft ceiling, paired t-tests assessed symmetry of the downdraft ceiling from the head of the table to corresponding location on the foot of the table, from the left side of the table to the corresponding location on the right side of the table, and from corner-to-corner (i.e., corresponding diagonal locations). Distribution of residuals was assessed by D'Agostino –Pearson tests (K^2) for normality.

To visualize the downdraft ceiling, a color-mapped matrix plot was produced. The matrix plot was subsequently interpolated and contoured. Then, a three-dimensional color-mapped surface plot of the downdraft ceiling was produced, and vantage points were manipulated to improve the two-dimensional representation of the three-dimensional downdraft ceiling using PAST 4 Statistical Software.

Results

The in-line duct fans generated airflows of 440, 486, 505, 500, and 440 m^3/h, for a total of 2371 m^3/h of downdraft airflow. Results of the varied aerosol downdraft visualizations were as follows:

1. Water vapor produced from condensation occurring post-sublimation of dry ice:

Without downdraft, the water vapor poured over each of the four boundaries of the downdraft tabletop, regardless of the position of the dry-ice container (Figure 3; Video 1[a]). With downdraft, and regardless of position, the water vapor did not cross any boundary of the tabletop (Figure 3; Video 1). Rather, the visible water vapor was confined to the proximity of the dry ice container.

2. Aerosolized 35% triethylene glycol + water mixture from fog machines:

Without downdraft, the fog machines produced a haze that escaped the perimeter of the table and rapidly filled the room, regardless of fog machine orientation (Figure 4; Video 2, Video 3, Video 4, and Video 5). The fog also traveled above the table to reach the ceiling of the room. With downdraft, the fog did not cross any boundary of the table, with the exception of the fog directed across the width of the table (Figure 4; Video 4). However, in the aforementioned circumstance, the fog that crossed the perimeter of the table was pulled backward, within the limits of the table, and flowed into the table (Video 4). Therefore, all of the fog produced was rapidly exhausted through the downdraft table.

3. Aerosolized glycerin + water mixture from a hand-held fog generator:

Without downdraft, well-defined aerosol plumes traveled directly upward, away from the surface of the table (Figure 5; Video 6). Conversely, with downdraft, the fog dissipated as it was pulled down and into the table (Figure 5; Video 6).

4. Cool water vapor generated from an ultrasonic air humidifier:

Without downdraft, plumes of water vapor arced over and beyond the perimeter of the downdraft table (Figure 6; Video 7). With downdraft, the water vapor plumes, reversed their direction toward the center of the table and the height of the water vapor plumes decreased, relative to the plumes seen in the absence of downdraft (Figure 6; Video 7).

[a] Full video permalinks are cited in the "Literature Cited." See Zdilla et al., 2022a-g. Video permalinks are also included in the appendix titled "Video Supplements." Hyperlinks direct to videos hosted by the Figshare data repository. All videos are in real-time. All videos are licensed under the creative commons license CC BY 4.0.

Figure 3: A side-by-side demonstration of the capacity of a simple downdraft table paired with a simple local exhaust ventilation system to exhaust water vapor (generated by pouring warm water into a container of frozen carbon dioxide). Images were captured from video 10 seconds after the addition of the water in the absence of downdraft (left column). In the absence of downdraft, water vapor rapidly escaped the perimeter of the downdraft table. In the presence of downdraft (right column), the downdraft table removed water vapor consistently and prevented water vapor from moving along the tabletop surface. Accordingly, the downdraft prevented the water vapor from escaping the perimeter of the table. **(A)** Dry-ice container located in the center of the table. **(B)** Dry-ice container located away from the exhaust manifold. **(C)** Dry-ice container located near the exhaust manifold. **NOTE:** This Figure corresponds to Video 1.

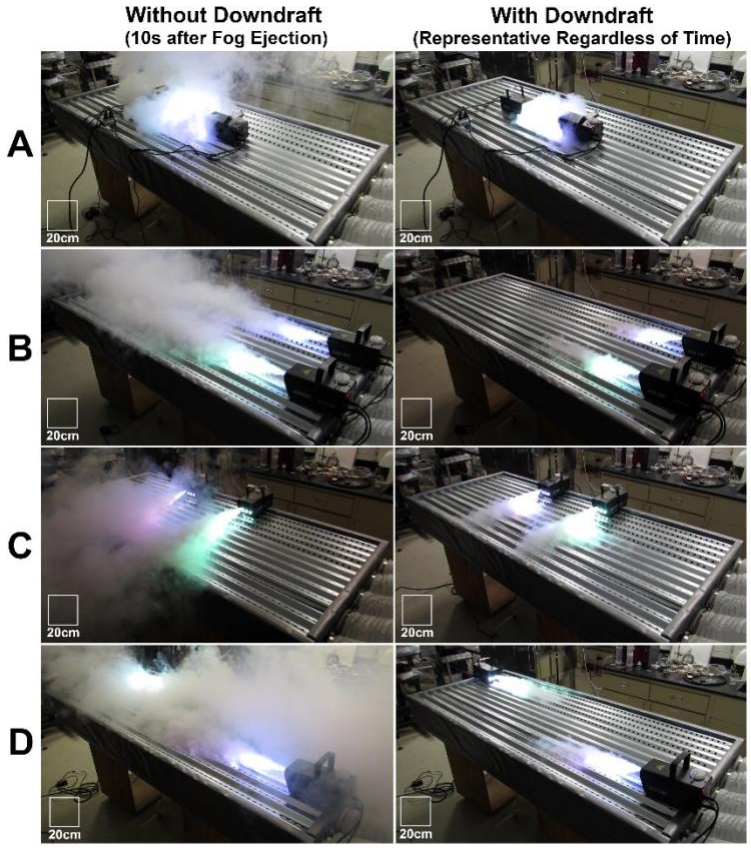

Figure 4: A side-by-side demonstration of the capacity of a simple downdraft table paired with a simple local exhaust ventilation system to exhaust a fog, composed of triethylene glycol and water, sprayed in varied directions from fog machines. Images were captured from video 10 seconds after fog ejection in the absence of downdraft (left column). In the absence of downdraft, fog rapidly escaped the perimeter of the downdraft table and rapidly filled the room with fog. In the presence of downdraft (right column), the downdraft table removed fog consistently and limited the spread of fog along the tabletop surface. Accordingly, the downdraft prevented the vapor from escaping the perimeter of the table. **(A)** Fog machines directed toward one another in the center of the downdraft table **(B)** Fog machines directed along the length of the downdraft table. **(C)** Fog machines directed along the width of the table. In this case, fog occasionally sprayed beyond the perimeter of the table. However, fog that moved beyond the table was immediately pulled back within the boundary of the table. Thus, no fog escaped the downdraft of the table. **(D)** Fog machines oriented anti-parallel along the length of the table. **NOTE:** This figure corresponds to Video 2, Video 3, Video 4, and Video 5.

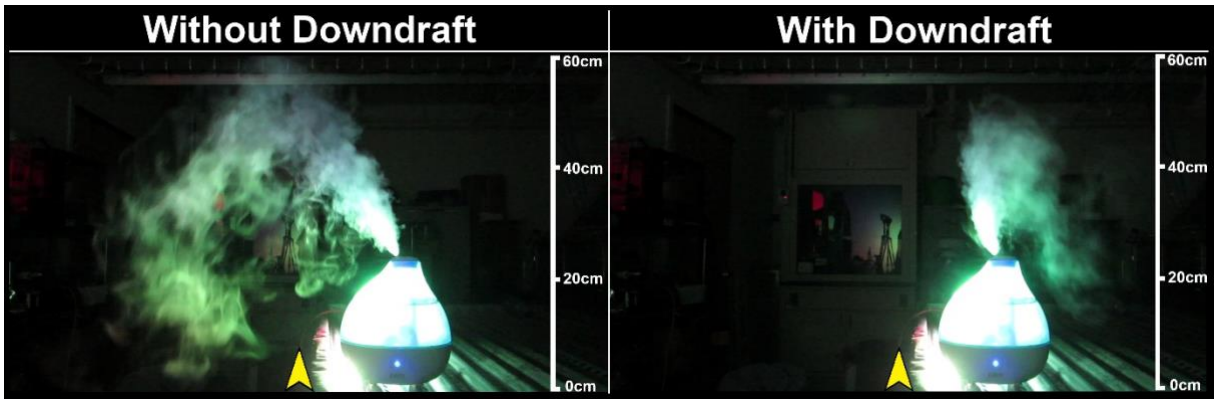

Figure 5: A side-by-side demonstration of the capacity of a simple downdraft table paired with a simple local exhaust ventilation system to exhaust a fog, composed of glycerin and water, emitted from a hand-held fog machine. NOTE: This figure corresponds to Video 6.

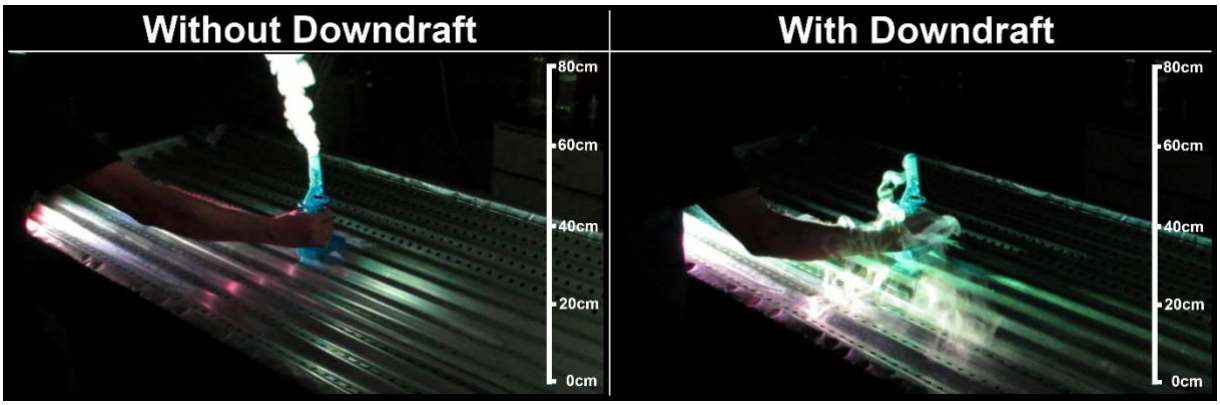

Figure 6: A side-by-side demonstration of the capacity of a simple downdraft table paired with a simple local exhaust ventilation system to prevent vaporized water, blown from an ultrasonic humidifier, from escaping the perimeter of the downdraft table (arrowheads). The downdraft reversed the direction and decreased the height of the water vapor plume. Similarly, the downdraft compressed the volume occupied by the water vapor. **NOTE:** This figure corresponds to Video 7.

5. Fire and smoke produced from the combustion of matches:

In the presence of downdraft, a single lit match and a group of six lit matches could be completely inverted near the table (~3 cm) with the entirety of the flame directed downward toward (or into) the table (Figure 7). A single lit match was extinguished a few centimeters above the table. A group of six lit matches was extinguished at the surface of the table. Subsequently, smoke was pulled downward and was exhausted through the downdraft table. With a group of ten lit matches, some flames ascended the inverted matches when held ~3 cm above the table. When extinguished, smoke was exhausted by the downdraft system.

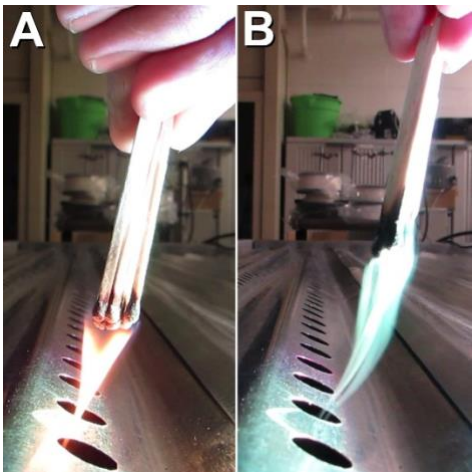

Figure 7: The downdraft table was able to **(A)** invert flames and **(B)** extinguish flames (when located in proximity to an opening in the tabletop), and exhaust smoke from extinguished flames.

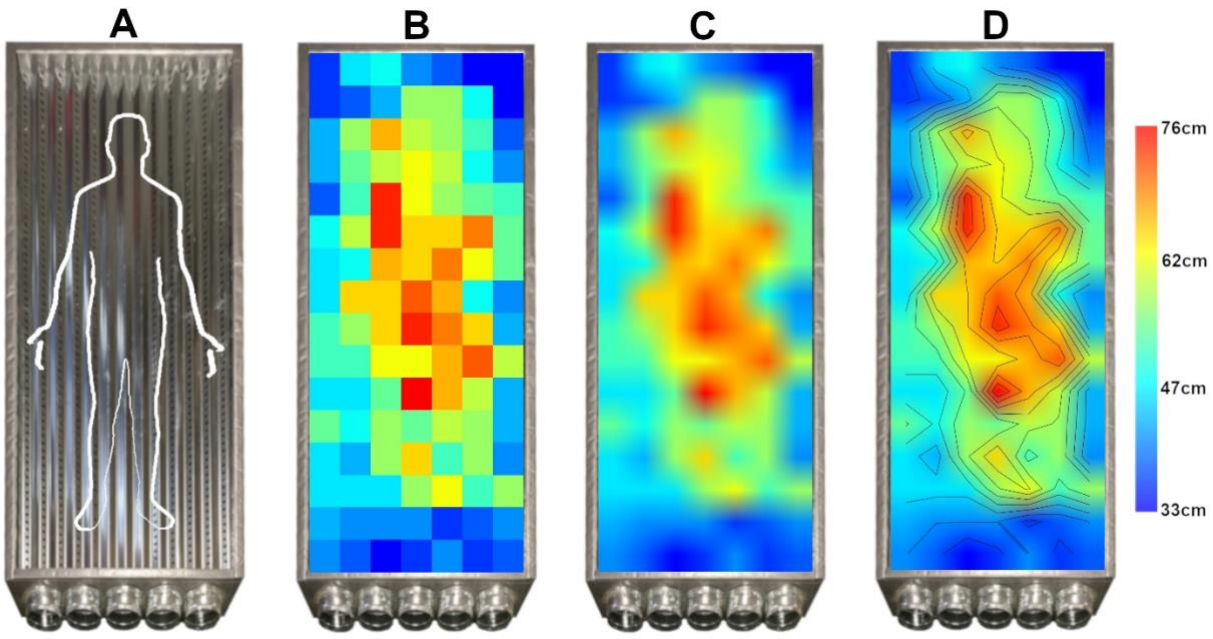

Figure 8: An overhead view of the downdraft table with a superimposed matrix plot that represents the downdraft ceiling distribution. The downdraft ceiling was highest in the center of the tabletop, represented by warm hues, and lowest along the perimeter of the tabletop, represented by cold hues. **(A)** Galvanized corrugated steel tabletop surface seen with a superimposed outline of an adult male of average stature (~176 cm in height). **(B)** Matrix plot. **(C)** Interpolated matrix plot. **(D)** Interpolated matrix plot with contours.

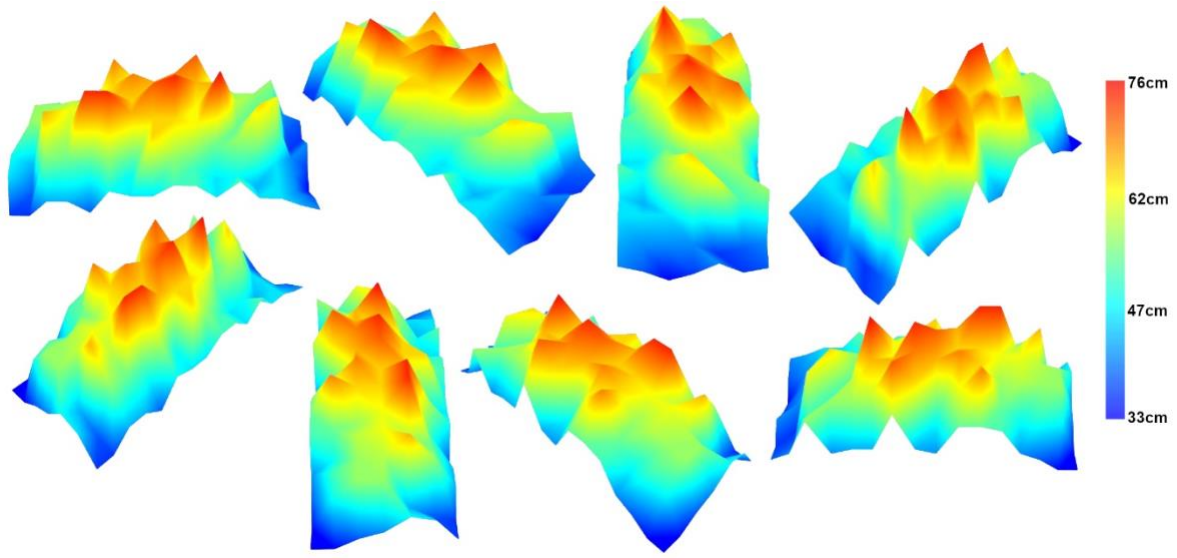

Figure 9: A three-dimensional surface plot representing the downdraft ceiling. All perspectives are from a 45° elevation. The azimuth changes clockwise and sequentially by 45° (e.g., the upper left image has an azimuth of 0°, the upper right image has an azimuth of 135°, the lower right image has an azimuth of 180°). The plots are oriented in a manner where the downdraft exhaust manifold would be oriented toward the center of the image. The downdraft ceiling is highest in the center, lowest at the perimeter, and statistically symmetrical from end-to-end and side-to-side. Furthermore, the downdraft ceiling has a relatively smooth gradation from the center to the periphery.

6. A three-dimensional downdraft ceiling with smoke generated from the combustion of a cellulose / stearic acid wick:

The downdraft table was capable of preventing upward movement of the smoke emanating from the Smoke Pen from a minimum of 33 cm and a maximum of 76 cm above the table. The highest downdraft ceiling was centralized whereas the lowest ceiling was located around the perimeter of the table and especially near the exhaust manifold and at the opposite corners of the table (Figures 8 and 9).

With regard to the symmetry of the downdraft ceiling, a paired t-test identified no significant differences between the head and foot of the table ($t=1.2(55)$, $p>0.05$) with normally distributed residuals ($K^2=0.78$; $p>0.05$). Paired t-test results identified no significant difference between left and right sides of the table ($t=0.96(47)$; $p>0.05$) with normally distributed residuals ($K^2=1.6$; $p>0.05$). Likewise, paired t-test results identified no significant difference between corner-to-corner / corresponding diagonal locations on the table ($t=1.3(55)$, $p>0.05$) with normally distributed residuals ($K^2=1.8$; $p>0.05$)

Discussion

The results of this study provide evidence that the utilization of an inexpensive, easy-to-build, readily portable, downdraft table, made of widely available materials, can be effectively paired with a simple local exhaust ventilation system to limit aerosols that are similar to those found in the clinical environment. Thus, in addition to increasing airflow and the number of air exchanges in a negative flow room, the local evacuation of aerosols from the downdraft table can decrease harmful spread of airborne pathogens in the vicinity of a recumbent patient. The relatively low cost and simple design of the downdraft table and exhaust system supports accessibility. Further, the table may be assembled rapidly and used in remote locations, quarantine scenarios, hospital patient overflow scenarios, household use, etc. to limit the spread of aerosolized pathogens.

Klompas et al (2021) recently suggested four factors to explain airborne transmission risk with regard to aerosol-generating procedures: 1) forced air— procedures that increase velocity and volume of air over a respiratory mucosa increases transmission risk; 2) symptoms and severity— coughing, sneezing, and heavy breathing increase the risk of transmission; 3) distance— respiratory emissions are densest closest to their source and further one gets from the source, the more time and space there is for respiratory emissions to diffuse and dilute in the surrounding air; and 4) duration— the longer one is exposed to a pathogenic aerosol, the greater the probability of infection. These four factors should be considered with regard to the utility of the exhaust ventilation demonstrated in this study. In particular, the downdraft table and local exhaust ventilation have particular value for any scenarios where there is increased velocity / volume of air leaving the body, which includes the many signs of disease (i.e., coughing, sneezing, etc.). Also, the downdraft table and local exhaust ventilation system can also prevent aerosols from traveling away from their source. Moreover, the exhaust is strongest nearest the source of the aerosol where the pathogen is found in the greatest density.

Models of water volume lost to exhalation during physical exertion have been calculated at 60-70 ml/h at a heart rate of 140bpm, four times higher than the water lost at rest (Zieliński and Przybylski, 2012). In comparison, this study tested relatively larger quantities of water vapor, for example, 150ml/hr, blown away from the tabletop by a small fan (Figure 6, Video 7). However, the dynamics of aerosol-generating procedures vary and are difficult to accurately recreate (Patel et al., 2020), and are thus only loosely approximated by the multifaceted approach of this study. Accordingly, this study approximated quiet breathing with the utilization of dry ice and the hand-held fog machine (Figures 3 and 5; Video 1 and Video 6). Exertional breathing was approximated with the ultrasonic humidifier (150 ml/hr) (Figure 6; Video 7) as well as fog machines, which also served to approximate non-respiratory air movements (Figure 4; Video 2, Video 3, Video 4, and Video 5). Surgical smoke plumes were approximated with the hand-held fog machine (Figure 5; Video 6), smoke generated from extinguished flames (Figure 7), and smoke from a smoke pen (Figure 2). Therefore, the results of this study provide evidence that the downdraft table and local exhaust ventilation system can limit the spread of aerosols that are found in varied clinical scenarios. The multifaceted

approach of this study provides a robust assessment of exhaust ventilation capability which, as the results of this report demonstrate, has broad application.

With regard to VOCs found in surgical smoke plumes, a local exhaust ventilation system which generated an exhaust flow of 1320 m^3/h was paired with a TBJ Model 32-86 DD-AT-M-AH downdraft table (TBJ Inc., Chambersburg, PA) and removed all airborne formaldehyde (0.00ppm) from a 1000ml pool of 100% formalin located 20cm above the table surface (Zdilla, 2021). Another study identified the complete removal of airborne VOCs emanating from a cadaver embalmed with Carolina's Perfect Solution® Concentrate with Phenol (Carolina Biological Supply Company, Burlington, NC), composed of alcohol, aldehyde, and phenol using the TBJ Model 32-86 DD-AT-M-AH downdraft table with a local exhaust ventilation system that produced 800 m^3/h. Klein et al (2014) reported a downdraft table, similar to the TBJ Model 32-86 DD-AT-M-AH downdraft table and made by TBJ Inc., that had an airflow of 467 m^3/h and effectively mitigated formaldehyde levels in the gross anatomy laboratory at Yale University. Thus, VOCs may be effectively exhausted from downdraft tables at flow rates at least five times lower than those measured in this study. Accordingly, fewer fans might have effectively removed aerosols in this study and thus conserved resources including fans, ducts, and electricity.

Regarding the aforementioned factors about airborne pathogen transmission risk per Klompas et al (2021), the amount of forced air / severity of symptoms and severity may influence the utility of local exhaust ventilation. Take, for example, a hypothetical quarantine scenario where six in-line duct fans were available for three individuals: one who is coughing/sneezing, one who was in close contact with the individual who has been coughing and sneezing, and one who was distanced from the other two. In such a scenario, perhaps it would be best to used three fans for the symptomatic patient, two for the exposed patient, and one for the patient with minimal exposure. By the same token, three fans may be ineffective at limiting aerosol transmission. This study used a consistent fan arrangement and downdraft flow. Thus, future studies should consider the relationship between varied exhaust flow and efficacy.

A prior study demonstrated that the downdraft table and local exhaust ventilation system (the same that was used in this study) could eliminate all airborne formaldehyde (0.00 ppm) from a 1000 ml pool of 100% formalin located 20 cm above the table surface (Zdilla, 2022). However, the study measured an airflow of 3099 m^3/h— greater than the 2371 m^3/h airflow measured in the present study. Because the table was the same and the fans were practically the same (apart from a variable speed controllers), the air flow difference can be attributed to the length and course of the flexible ducts. The ducts were longer, less-expanded due to their laxity in tension, and more tortuous in the present study compared to the former study. Furthermore, this study identifies lower flow from the ducts positioned nearest the sides of the downdraft table, which were more tortuous than the centrally positioned ducts, which were relatively straight. Thus, this study used an airflow that was sub-maximal, yet still demonstrated effective exhaust of aerosols. Accordingly, airflow can be increased by decreasing the resistance to flow using straight, short, and smooth (i.e., rigid as opposed to flexible) ducts. Likewise, airflow can be increased by using different configurations / amounts / types of in-line duct fans (Zdilla, 2021).

The table used in this study was originally designed for the removal of VOCs that emanate from embalmed cadavers. Thus, the openings in the table surface run from the head to the foot of the table. In regard to utility, select openings may be covered / eliminated and the inner "ramp" within the table adapted for varied uses— see design details in Zdilla (2022). For example, in the case of a patient who is coughing / sneezing, it would be desirable to have more downdraft near their face rather than at their feet. So, the inner ramp can be shortened and oriented more vertically, and surface openings can be covered with other sheets of corrugated steel or, alternatively, different surfaces with openings designed for specific purposes could be used. Thus, the table can be easily adapted for varied uses.

Acknowledgements

This work was supported by NIH R01 ES015022 (TN) and U54 GM104942.

Literature Cited

Alp E, Bijl D, Bleichrodt RP, Hansson B, Voss A. 2006. Surgical smoke and infection control. J Hosp Infect. 62(1):1-5. doi:10.1016/j.jhin.2005.01.014

Bhattacharjee HK, Chaliyadan S, Verma E, Ramachandran R, Makharia G, Parshad R. 2021. Coronavirus disease 2019 and laparoscopic surgery in resource-limited settings. Asian J Endosc Surg. 14(2):305-308. doi:10.1111/ases.12835

Donato G, Forti E, Mutignani M, et al. 2021. A multicenter survey on endoscopic retrograde cholangiopancreatography during the COVID-19 pandemic in northern and central Italy. Endosc Int Open. 9(4):E629-E634. doi:10.1055/a-1380-3419

Hellman S., Chen G.H., Irie T. 2020. Rapid clearing of aerosol in an intubation box by vacuum filtration. Br J Anaesth. 125:e296-e299.

Jain R, Kroboth S, Ignatowski D, Khandheria BK. 2021. Seroprevalence of SARS-CoV-2 Antibody in Echocardiography and Stress Laboratory. J Patient Cent Res Rev. 8(2):146-150.

Klein RC, King C, Castagna P. 2014. Controlling formaldehyde exposures in an academic gross anatomy laboratory. J Occup Environ Hyg 11:127–132.

Klompas M., Baker M., Rhee C. 2021. What Is an Aerosol-Generating Procedure?. JAMA Surg. 156:113-114.

Komperda J, Peyvan A, Li D, et al. 2021. Computer simulation of the SARS-CoV-2 contamination risk in a large dental clinic. Phys Fluids (1994). 33(3):033328. doi:10.1063/5.0043934

Lee T, Soo JC, LeBouf RF, et al. 2018. Surgical smoke control with local exhaust ventilation: Experimental study. J Occup Environ Hyg. 15(4):341-350. doi:10.1080/15459624.2017.1422082

Mowbray NG, Ansell J, Horwood J, et al. 2020. Safe management of surgical smoke in the age of COVID-19. Br J Surg. 107(11):1406-1413. doi:10.1002/bjs.11679

Occupational Safety and Health Administration. Surgical Suite. https://www.osha.gov/SLTC/etools/hospital/surgical/surgical.html

Patel SH, Yim W, Garg AK, Shah SH, Jokerst JV, Chao DL. 2020. Assessing the Physiological Relevance of Cough Simulators for Respiratory Droplet Dispersion. J Clin Med. 17;9(9):3002. doi: 10.3390/jcm9093002

Romanzi A, Gabaglio M, Milanesi M, et al. 2021. Pain distraction during awake low anterior resection and Cuddle Delivery initiative for inpatient: frugal procedural options to support surgery in the COVID-19 era. Eur Rev Med Pharmacol Sci. 25(7):3116-3121. doi:10.26355/eurrev_202104_25566

Sinnige JS, Kooij FO, van Schuppen H, Hollmann MW, Sperna Weiland NH. 2021. Protection of healthcare workers during aerosol-generating procedures with local exhaust ventilation [published online ahead of print, 2021 Mar 20]. Br J Anaesth. S0007-0912(21)00166-5. doi:10.1016/j.bja.2021.02.032

Tkacik PT, Dahlberg JL, Johnson JE, Hoth JJ, Szer RA, Hellman SE. 2021. Sizing of airborne particles in an operating room. PLoS One. 16(4):e0249586.

Ulmer BC. 2008. The hazards of surgical smoke. AORN J. 87(4):721-738. doi:10.1016/j.aorn.2007.10.012

Weiland NHS, Traversari RAAL, Sinnige JS. 2021. Influence of room ventilation settings on aerosol clearance and distribution. Br J Anaesth. 126:E49–E52

Wilson NM, Marks GB, Eckhardt A, et al. 2021. The effect of respiratory activity, non-invasive respiratory support and facemasks on aerosol generation and its relevance to COVID-19 [published online ahead of print, 2021 Mar 30]. Anaesthesia. 2021;10.1111/anae.15475. doi:10.1111/anae.15475

Zdilla MJ. 2020. Creating a Human Gross Anatomy Laboratory: The Experience at a Primarily Undergraduate Institution. Anat Sci Educ. 13(5):636-647. doi:10.1002/ase.1946

Zdilla MJ. 2021. Local exhaust ventilation systems for the gross anatomy laboratory. Morphologie. 105(350):237-246. doi: 10.1016/j.morpho.2020.11.002.

Zdilla MJ. 2022. Creating an inexpensive yet effective downdraft table for a gross anatomy laboratory: Proof-of-concept. Morphologie. 106(352):28-36. doi: 10.1016/j.morpho.2021.02.009.

Zdilla MJ, Goldsmith WT, Nurkiewicz TR. 2022a. Removal of an Aerosolized 35% Triethylene Glycol and Water Mixture from Fog Machines Directed Along the Width of a Novel Downdraft Table (Version 1). figshare. https://doi.org/10.6084/m9.figshare.19890250.v1

Zdilla MJ, Goldsmith WT, Nurkiewicz TR. 2022b. Removal of an Aerosolized 35% Triethylene Glycol and Water Mixture from Fog Machines Directed Anti-Parallel Along the Length of a Novel Downdraft Table (Version 1). figshare. https://doi.org/10.6084/m9.figshare.19890247.v1

Zdilla MJ, Goldsmith WT, Nurkiewicz TR. 2022c. Removal of an Aerosolized 35% Triethylene Glycol and Water Mixture from Fog Machines Directed Parallel Along the Length of a Novel Downdraft Table (Version 1). figshare. https://doi.org/10.6084/m9.figshare.19890238.v1

Zdilla MJ, Goldsmith WT, Nurkiewicz TR. 2022d. Removal of an Aerosolized 35% Triethylene Glycol and Water Mixture from Fog Machines Directed Toward One Another in the Center of a Novel Downdraft Table (Version 1). figshare. https://doi.org/10.6084/m9.figshare.19890232.v1

Zdilla MJ, Goldsmith WT, Nurkiewicz TR. 2022e. Removal of an Aerosolized Glycerin and Water Mixture from a Hand-Held Fog Generator by a Novel Downdraft Table (Version 1).

figshare. https://doi.org/10.6084/m9.figshare.19890244.v1

Zdilla MJ, Goldsmith WT, Nurkiewicz TR. 2022f. Removal of Cool Water Vapor Generated from an Ultrasonic Air Humidifier by a Novel Downdraft Table (Version 1). figshare. https://doi.org/10.6084/m9.figshare.19890241.v1

Zdilla MJ, Goldsmith WT, Nurkiewicz TR. 2022g. Removal of Water Vapor Produced from Condensation Occurring Post-Sublimation of Dry Ice by a Novel Downdraft Table (Version 1). figshare. https://doi.org/10.6084/m9.figshare.19890235.v1

Zieliński J, Przybylski J. Ile wody tracimy z oddechem? [How much water is lost during breathing?]. Pneumonol Alergol Pol. 2012;80(4):339-342.

Video Supplements

Video 1:
https://doi.org/10.6084/m9.figshare.19890235.v1

Video 2:
https://doi.org/10.6084/m9.figshare.19890232.v1

Video 3:
https://doi.org/10.6084/m9.figshare.19890238.v1

Video 4:
https://doi.org/10.6084/m9.figshare.19890250.v1

Video 5:
https://doi.org/10.6084/m9.figshare.19890247.v1

Video 6:
https://doi.org/10.6084/m9.figshare.19890241.v1

Video 7:
https://doi.org/10.6084/m9.figshare.19890244.v1